AD-A119 035   NEW MEXICO STATE UNIV LAS CRUCES PHYSICAL SCIENCE LAB   F/G 9/5
               INPUT IMPEDANCE TO PROBE FED MICROSTRIP ANTENNAS OVER ELECTRICA--ETC(U)
               JUN 82   J VENKATARAMAN, D C CHANG, K R CARVER   DAAG29-81-K-0112
UNCLASSIFIED   NMSU/PSL-PI01001   ARO-15384.3-EL   NL

1 OF 1
AD A
119035

END
DATE
FILMED
10-82
DTIC

PSL Report No. PI01001

ARO 15384.3-EL
18448.1-EL
⑫

INPUT IMPEDANCE TO PROBE FED MICROSTRIP ANTENNAS

FINAL REPORT

by

Jayanti Venkatarman
Electromagnetics Research Group
Physical Science Laboratory
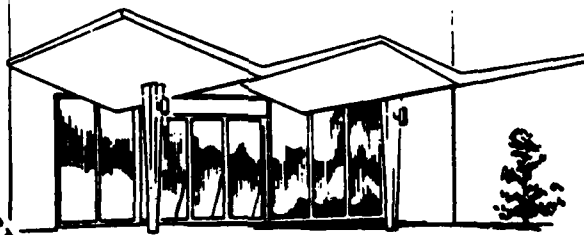New Mexico State University
Las Cruces, NM 88003

David C. Chang
Elecromagnetics Laboratory
Department of Electrical Engineering
University of Colorado
Boulder, CO 80309

Keith R. Carver
Jet Propulsion Laboratory
4800 Oak Grove Drive
Pasadena, CA 91109

Bruce A. Blevins
Electromagnetics Research Group
Physical Science Laboratory
New Mexico State University
Las Cruces, NM 88003

June 8, 1982

SEP 0 8 1982

E

Physical Science Laboratory

P.O. Box 3548, Las Cruces, NM 88003-3548
Area (505) 522-9100 TWX 910-983-0541

82 0 3

REPORT DOCUMENTATION PAGE		READ INSTRUCTIONS BEFORE COMPLETING FORM
1. REPORT NUMBER	2. GOVT ACCESSION NO. AD-A119 035	3. RECIPIENT'S CATALOG NUMBER
4. TITLE *(and Subtitle)* "Input Impedance to Probe Fed Microstrip Antennas over Electrically Thick Substrates".		5. TYPE OF REPORT & PERIOD COVERED Final; July 1, 1981 to June 8, 1982.
		6. PERFORMING ORG. REPORT NUMBER
7. AUTHOR(s) Jayanti Venkataraman, David Chang, Keith R. Carver, and Bruce Blevins.		8. CONTRACT OR GRANT NUMBER(s) DAAG29-81-K-0112
9. PERFORMING ORGANIZATION NAME AND ADDRESS Physical Science Laboratory Box 3548, Las Cruces, NM 88003		10. PROGRAM ELEMENT, PROJECT, TASK AREA & WORK UNIT NUMBERS
11. CONTROLLING OFFICE NAME AND ADDRESS U.S. Army Research Office Post Office Box 12211 Research Triangle Park, NC 27709		12. REPORT DATE June 8, 1982
		13. NUMBER OF PAGES 37
14. MONITORING AGENCY NAME & ADDRESS *(If different from Controlling Office)*		15. SECURITY CLASS. *(of this report)* Unclassified
		15a. DECLASSIFICATION/DOWNGRADING SCHEDULE

16. DISTRIBUTION STATEMENT *(of this Report)*

Approved for public release; distribution unlimited.

17. DISTRIBUTION STATEMENT *(of the abstract entered in Block 20, if different from Report)*

N/A

18. SUPPLEMENTARY NOTES

The view, opinions, and/or findings contained in this report are those of the author(s) and should not be construed as an official Department of the Army position, policy, or decision, unless so designated by other documentation.

19. KEY WORDS *(Continue on reverse side if necessary and identify by block number)*

Microstrip Patch Antenna Impedance.
Thick Substrate Microstrip Patch Antenna
Antenna Input Impedance

20. ABSTRACT *(Continue on reverse side if necessary and identify by block number)*

A general theory has been developed for the analysis of the input impedance to probe fed microstrip patch antennas where the entire spectrum of plane waves emanating from the exciting probe and an angularly dependent wall reflection coefficient has been incorporated.

DD FORM 1473 EDITION OF 1 NOV 65 IS OBSOLETE
1 JAN 73

20. ABSTRACT CONTINUED

The primary emphasis is toward millimeter wavelength microstrip patch antennas where the substrate is electrically thick and requires the consideration of the dispersive effects of the dielectric.

The expressions derived here for the input impedance are for a given probe location, size, and patch dimensions. The theory has no perceivable limitations with respect to substrate thickness or patch dimensions.

Numerical results have been presented and compared with those obtained by the cavity model (reference [10] in this report). A discussion of these results points out the primary feature of the present theoretical models, in that the wall susceptance being dynamic in nature, the expression obtained for input impedance is more appropriate for millimeter microstrip antennas. Comparison of this theory to experiment (reference [11]) shows that this theory properly incorporates high frequency effects on the open end susceptance of a microstrip patch antenna.

PROGRESS REPORT NUMBER 1

(TWENTY COPIES REQUIRED)

1. ARO PROPOSAL NUMBER: _____81-ARO-132_____

2. PERIOD COVERED BY REPORT: ___July 1, 1981 to June 8, 1982.___

3. TITLE OF PROPOSAL: ___Theoretical Investigation of a Combined___
   ___Modal Expansion and Wiener-Hopf Theory for the Microstrip___
   ___Patch Antenna.___

4. CONTRACT OR GRANT NUMBER: _____DAAG29-81-K-0112_____

5. NAME OF INSTITUTION: _____Physical Science Laboratory_____
   _____P.O. Box 3548_____
   _____Las Cruces, NM 88003-3548_____

6. AUTHOR(S) OF REPORT: ___Jayanti Venkataraman, David Chang,___
   ___Bruce Blevins, and Keith R. Carver.___

7. LIST OF MANUSCRIPTS SUBMITTED OR PUBLISHED UNDER ARO SPONSORSHIP
   DURING THIS PERIOD, INCLUDING JOURNAL REFERENCES:

   Carver, K.R. and Venkataraman, J., "Input Impedance to Micro-
   strip Antennas over Thick Substrates", Digest National Radio
   Science Meeting, Boulder, CO, January 1981, pp. 123.

8. SCIENTIFIC PERSONNEL SUPPORTED BY THIS PROJECT AND DEGREES AWARDED
   DURING THIS REPORTING PERIOD:

   Jayanti Venkataraman, post-doctoral student.

BRIEF OUTLINE OF RESEARCH FINDINGS

This investigation has resulted in the development of a set
of generalized equations for calculating the input impedance
to a microstrip patch antenna over a thick substrate.

The primary application of this theory is for millimeter
wavelength microstrip antennas where the substrate can be
electrically thick and requires consideration of the disper-
sion effects of the dielectric.

The results of the investigation are compared to the cavity
or modal theory for the input impedance to a thin substrate
and to experimentaily determined input impedances. Excellent
agreement is found for these geometrics.

INPUT IMPEDANCE TO PROBE FED MICROSTRIP ANTENNAS

FINAL REPORT

by

Jayanti Venkatarman
Electromagnetics Research Group
Physical Science Laboratory
New Mexico State University
Las Cruces, NM 88003

David C. Chang
Elecromagnetics Laboratory
Department of Electrical Engineering
University of Colorado
Boulder, CO 80309

Keith R. Carver
Jet Propulsion Laboratory
4800 Oak Grove Drive
Pasadena, CA 91109

Bruce A. Blevins
Electromagnetics Research Group
Physical Science Laboratory
New Mexico State University
Las Cruces, NM 88003

prepared for the

U.S. Army Research Office
Research Triangle Park, NC

Contract No. DAAG29-81-K-0112

June 8, 1982

Preface

The work summarized in this report is the result of a one year study sponsored by the U.S. Army Research Office (Contract DAAG29-81-K-0112) on the theoretical analysis of input impedance to millimeter wave microstrip antennas. The work performed as a joint effort between the Electromagnetics Research Group at the Physical Science Laboratory, New Mexico State University and the Electromagnetics Laboratory at the Department of Electrical Engineering, University of Colorado, Boulder. The effort was led by Dr. Venkataraman, a PSL Post-Doctoral Intern, who was in residence at the Department of Electrical Engineering, University of Colorado during the theoretical development phase. The Physical Science Laboratory wishes to express its appreciation to the Department of Electrical Engineering, University of Colorado, and to Dr. David Chang in particular for very significant contributions to this project.

Contents

Illustrations

1.0 INTRODUCTION

This report presents an improved theory for the analysis of input impedance of a probe-fed microstrip patch antenna. The motivation of this work arises from the need for a more accurate determination of the characteristics of millimeter microstrip antennas than obtainable from currently available cavity and transmission line models. A complete spectrum representation of a probe excited microstrip antenna has been developed based on the work of Chang and his colleagues [1,3], where the cavity wall reflection coefficient has been obtained as a function of the angle of incidence of interior waves bouncing between the walls.

The first mathematical model of the basic microstrip radiator used a one-dimensional transmission line analogy [4,5] and were later extended to two dimensions by the cavity model [6-8]. However, neither of these theories account for the dispersion effects caused by the grounded dielectric slab. Of particular interest here is the background work of the modal field expansion theory [6]. This theory is based on the conventional Fourier series expansion of the fields inside the cavity formed by the microstrip patch and its associated ground plane. In its present form it assumes a thin cavity so that the interior fields are composed of discrete modes which may be calculated assuming a fixed angularly independent wall reflection coefficient. The effect of radiation is represented in terms of an increased substrate loss tangent as done by Lo et. al. [6] or by the method of impedance boundary condition at the wall by Carver et. al. [8]. When the electrical thickness of the cavity ranges from 0.02 to 0.2 as in the case of practical microstrip antennas in the L, S or C band regions, the surface waves supported by the dielectric substrate carry relatively little power and the assumption of a perfect magnetic wall and an angularly independent reflection coefficient for any given patch geometry and frequency of operation is fairly reasonable.

By contrast, microstrip patch antennas constructed with commercially available substrate thicknesses and operated at the X-band or higher frequencies may have an electrical thickness equal to and exceeding 0.5. Experimental results obtained with the X-band patch antennas [9] show that the cavity theory breaks down as the substrate becomes electrically thicker since an appreciable amount of input power is transferred to surface waves on the open grounded substrate.

1

This inadequacy of the cavity theory underscores the need for a better theoretical description of millimeter wave microstrip antennas.

The analysis of the microstrip patch antenna by Change, Chang and Kuester [1,2] is based on the recognition that the natural modes of the antenna are established on transverse resonance conditions which incorporate the angularly dependent reflection coefficient associated with the cavity walls. This angular dependence is a direct result of the surface waves and radiation supported by the grounded dielectric substrate. The Wiener-Hoff technique has been used to find the reflection coefficient and the analyses has been used to compute the optimum range of patch side length aspect ratios in the sense of low Q or greatest bandwidth.

The present theory considers the complete spectrum of plane waves propagating from the excitation probe at all angles. The natural modes are established on the same transverse resonance condition obtained by Chang which incorporates the angularly dependent reflection co-efficient associated with the patch boundaries. The reactive part of the probe impedance for a truncated rectangular patch is due to the evanescent waves which are usually confined to the vicinity of the probe. Those directed at specific angles interfere constructively and propagate down the strip without decay. These are the guiding modes and the corresponding edges of the patch act as the non-radiating walls. Some of the spectrum propagation will leak out at the edges of the patch in the form of radiation.

This report presents the theoretical analysis of input impedance to probe fed microstrip patch antennas. Expressions have been obtained as a function of patch size, probe location and size and frequency of operation.

2.0 INFINITELY EXTENDING MICROSTRIP PATCH ANTENNA

2.1 Geometry of the Problem

The analysis has been broken into two phases. In the first phase, the micro-strip patch antenna has been considered as infinitely extending in the x direction as shown in Figure 1. The width of the patch is ℓ in the y direction. It is excited by a z-directed probe located at (x_0, y_0). The patch is located on the surface of a grounded dielectric slab of thickness d and relative permittivity ε_r. This then allows us to view the structure as an infinitely extending waveguide and helps us to establish all waves both propagating and evanescent which emanate from the exciting probe at different angles.

The evanescent waves directed at different angles would decay very quickly within a small distance from the probe and would account for the reactive part of the input impedance (Figure 2a). Some of these waves may reach out to the walls in the x direction where they could partially leak out as spurious radia-tion and also be partially reflected in the y direction.

The propagating modes bounce back and forth in the y direction (Figure 2b), either interfering constructively or destructively. Only those directed at specific angles interfere constructively and propagate down the patch as guiding modes. They ultimately characterize the resonant properties of the patch. The others which interfere destructively leak out as spurious radia-tion in the y direction as the waves progress along the x direction.

Hence an analysis of an infinite patch would help establish the transverse resonance condition for the guided modes and the entire spectrum of plane waves emanating from the source. In the second phase of the analysis, we consider a truncated patch which results in waves bouncing in the x direction. The input impedance of such a finite patch can then be calculated from the electric field.

2.2 Field Under the Infinite Microstrip Patch

We first assume the electric current density due to the filamentary exciting probe source is of the form
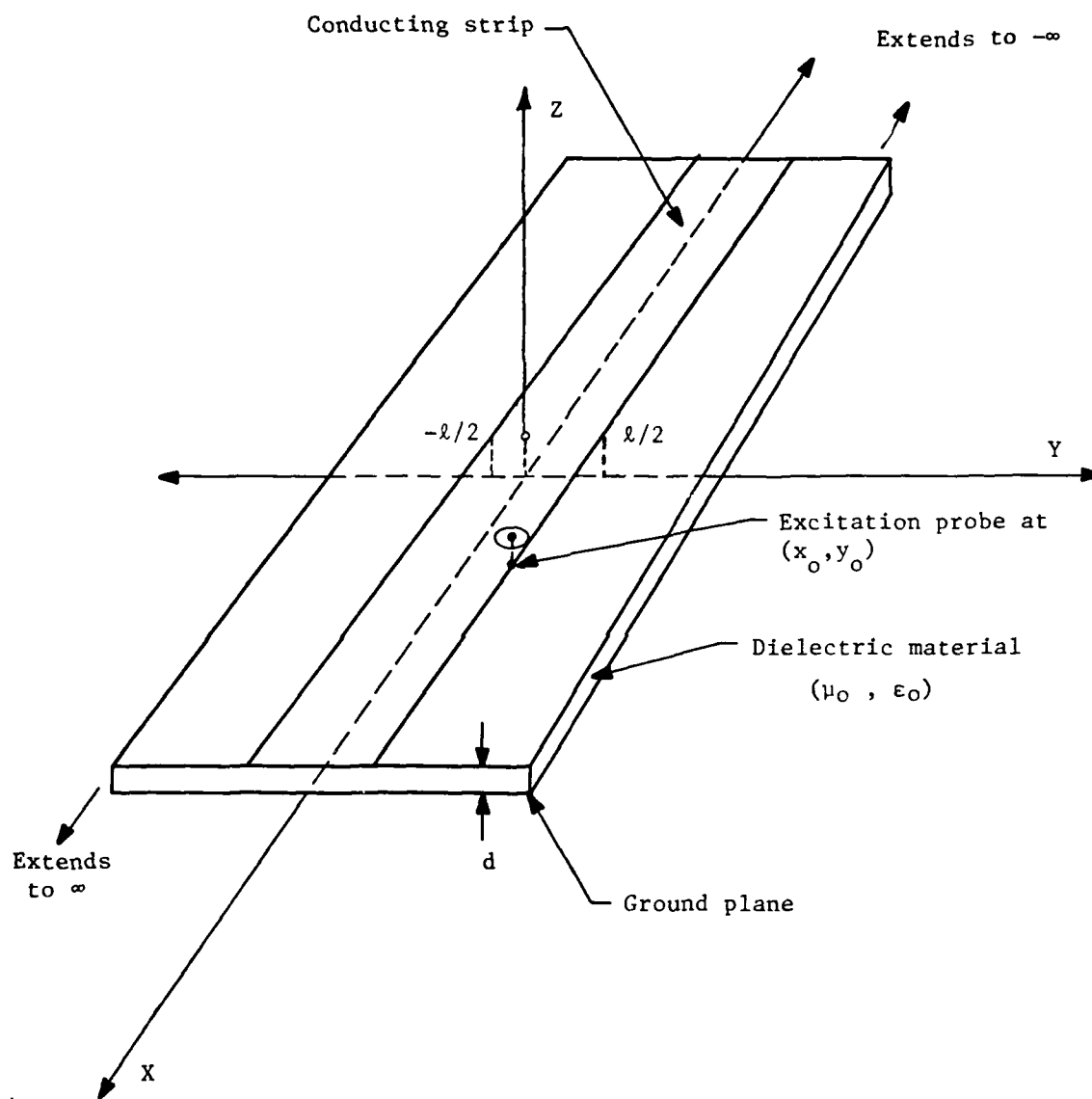
3

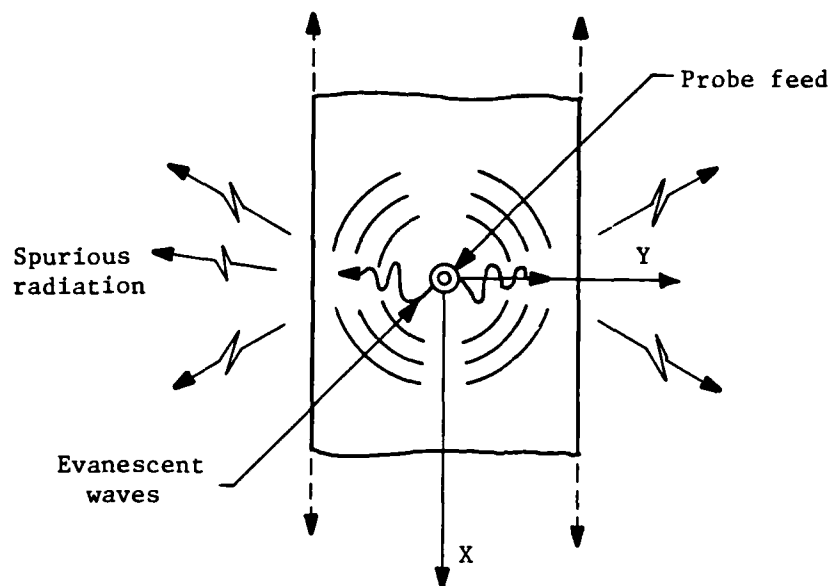Fig. 1.   Infinitely long probe-fed microstrip patch antenna.

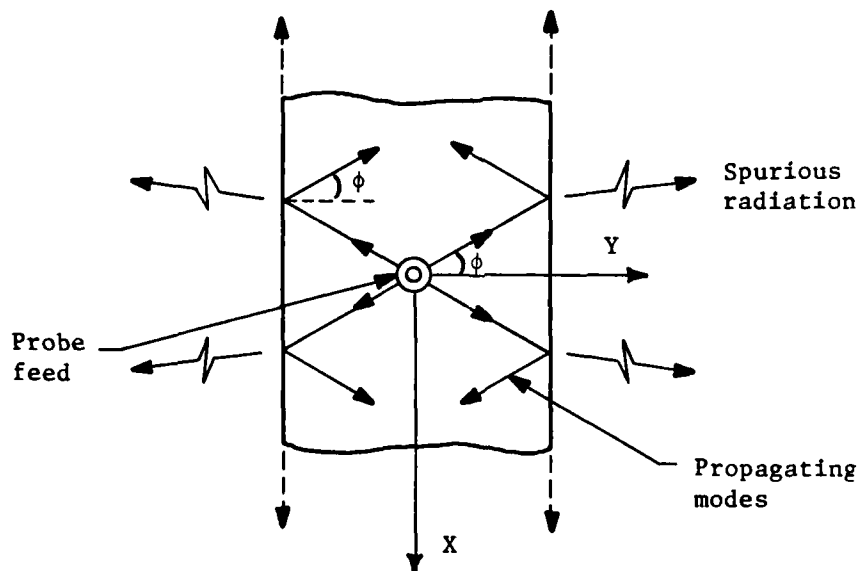Fig. 2a. Evanescent waves emanating from the exciting probe.

Fig. 2b. Propagating modes interfering constructively and destructively.

5

$$\vec{J} = I \; \hat{a}_z \; \delta(x - x_o) \; \delta(y - y_o) \tag{1}$$

The primary z-directed electric field emanating from the probe then satisfies the wave equation

$$\left(\frac{d^2}{dx^2} + \frac{d^2}{dy^2} + k^2 n^2\right) E_z = - i\omega\mu \; I \; \delta(x - x_o)\delta(y - y_o) \tag{2}$$

where $n^2 = \mu_r \epsilon_r$ and $k^2 = \omega^2 \mu_o \epsilon_o$ and where the assumed but suppressed time variation is exp $(-i\omega t)$. It is well-known that the solution of eq. (2) can be represented by a spectrum of plane waves of the general form:

$$E_z = \frac{k}{2\pi} \int_{\infty}^{\infty} d\alpha \; e^{ik\alpha(x_> - x_{o<})} \; \tilde{E}_z \; (y, \; \alpha) \tag{3}$$

A specific solution of eq. (2) is

$$E_z = A_o \int_{-\infty}^{\infty} e^{ik\alpha(x_> - x_{o<})} e^{ik\sqrt{n^2 - \alpha^2} \; (y_> - y_{o<})} \; \frac{d\alpha}{\sqrt{n^2 - \alpha^2}} \tag{4}$$

where $y_> \genfrac{}{}{0pt}{}{=}{\gtrless} \genfrac{}{}{0pt}{}{max}{min} (y, \; y_o)$ and $x_> \genfrac{}{}{0pt}{}{=}{\gtrless} \genfrac{}{}{0pt}{}{max}{min} (x, \; x_o)$

α = constant

$$A_o = \frac{-\omega\mu \; I}{4\pi} \tag{5}$$

Eq. (4) represents an angular spectrum of plane waves, or primary waves from the probe. The exponential term in the integral (4) can be written for propagating (non-evanescent) waves as

$$e^{iknr} = e^{ik[\alpha(x_> - x_{o<}) + \sqrt{n^2 - x^2} \; (y_> - y_{o<})]}$$

6

where r is the radial distance from the probe and $\alpha = n \cos \phi$ with the angle ϕ defined as shown in Figure 26. However, α is in general complex since evanescent waves are also possible.

Reflection occurs as these primary waves are incident on the two edges of a microstrip of finite width. For an infinitely long patch the waves travelling in the x direction while bouncing in the y direction would be the sum of incident waves, those which travel in the positive y direction and those which travel in the negative y direction. Hence we can write

$$E_z = A_0 \int_{-\infty}^{\infty} e^{ik\alpha(x-x_0)} \left[e^{ik\sqrt{n^2-\alpha^2}\,(y-y_0)} + A\,e^{ik\sqrt{n^2-\alpha^2}(\ell/2-y)} \right. $$
$$\left. + B\,e^{ik\sqrt{n^2-\alpha^2}\,(y+\ell/2)} \right] \frac{d\alpha}{\sqrt{n^2-\alpha^2}} \tag{6}$$

The amplitude A of waves reflected from the edge at $y = \ell/2$ can be determined by the boundary condition imposed at the edge:

$$A = \left[e^{-ik\sqrt{n^2-\alpha^2}\,y_0} + B\,e^{ik\sqrt{n^2-\alpha^2}\,\ell/2} \right] \Gamma(\alpha)\,e^{ik\sqrt{n^2-\alpha^2}\,\ell/2} \tag{7}$$

where $\Gamma(\alpha)$ is the complex reflection coefficient obtained in [2]. Similarly, the amplitude B is given by the edge condition at $y = -\ell/2$ as

$$B = \left[e^{ik\sqrt{n^2-\alpha^2}\,y_0} + A\,e^{ik\sqrt{n^2-\alpha^2}\,\ell/2} \right] \Gamma(\alpha)\,e^{ik\sqrt{n^2-\alpha^2}\,\ell/2} \tag{8}$$

Solving for A and B, the sum of the second and third terms in eq. (6) would be given as follows

$$Ae^{ik\sqrt{n^2-\alpha^2}\,(\ell/2 - y)} + Be^{ik\sqrt{n^2-\alpha^2}\,(y + \ell/2)}$$

$$= \frac{\Gamma(\alpha)\ e^{ik\sqrt{n^2-\alpha^2}\ell}}{1-\Gamma^2(\alpha)e^{i2k\sqrt{n^2-\alpha^2}\ell}}\left[e^{-ik\sqrt{n^2-\alpha^2}y}\left\{e^{-ik\sqrt{n^2-\alpha^2}y_0}\right.\right.$$

$$+ \Gamma(\alpha)e^{ik\sqrt{n^2-\alpha^2}\ell}\ e^{ik\sqrt{n^2-\alpha^2}\ y_0}\Big\} + e^{ik\sqrt{n^2-\alpha^2}y}\left\{e^{ik\sqrt{n^2-\alpha^2}\ y_0}\right.$$

$$\left.\left. + \Gamma(\alpha)e^{ik\sqrt{n^2-\alpha^2}\ell}\ e^{-ik\sqrt{n^2-\alpha^2}y_0}\right\}\right] \tag{9}$$

$$= \frac{\Gamma(\alpha)e^{ik\sqrt{n^2-\alpha^2}\ell}}{\Delta}\left[\cos\!\left(k\sqrt{n^2-\alpha^2}(y+y_0)\right) + \Gamma(\alpha)\ e^{ik\sqrt{n^2-\alpha^2}\ell}\ \cos\!\left(k\sqrt{n^2-\alpha^2}(y-y_0)\right)\right] \tag{10}$$

where

$$\Delta = 1 - \Gamma^2(\alpha)\ e^{i2k\sqrt{n^2 - \alpha^2}\ \ell} \tag{11}$$

Substituting in eq. (6) we have

$$E_z = A_0 \int_{-\infty}^{\infty}\frac{d\alpha}{\sqrt{n^2-\alpha^2}}\ e^{ik\alpha(x-x_0)}\left[e^{ik\sqrt{n^2-\alpha^2}\ (y-y_0)}\right.$$

$$+ \frac{2\ \Gamma(\alpha)}{\Delta}\ e^{ik\sqrt{n^2-\alpha^2}\ell}\ \left\{\cos\!\left(k\sqrt{n^2-\alpha^2}(y+y_0)\right) + \Gamma(\alpha)e^{ik\sqrt{n^2-\alpha^2}\ell}\right.$$

$$\left.\left. \times\ \cos\!\left(k\sqrt{n^2-\alpha^2}(y-y_0)\right)\right\}\right] \tag{12}$$

8

2.3 Angularly Dependent Reflection Coefficient

As mentioned earlier, $\Gamma(\alpha)$ is the complex reflection coefficient of the
plane waves bouncing in the y direction. When the plane waves from the
exciting probe proceed in the y direction at different angles, whether
these waves radiate into open space or not depends on the angle of incidence.
A complete reflection is possible if the angle of incidence $\phi = \sin^{-1}(\alpha/n)$
where n is the refractive index, is greater than some critical angle. Beyond
this critical angle the reflection coefficient has a magnitude of unity.
The reflection coefficient was obtained by Chang and Kuester [2] using the
Weiner-Hopf technique as applied to coupled integral equations for charge
and longitudinal distributions on the patch. An analytical expression obtained
by them [3] for thin slabs is given by

$$\Gamma(\alpha) = e^{-ix(\alpha)} \tag{13}$$

where

$$\chi(\alpha) = 2 \tan^{-1}\left(\frac{\alpha}{\sqrt{n^2-\alpha^2}} \tanh(\Delta)\right) - f_e(-\sqrt{n^2-\alpha^2}) \tag{14a}$$

$$\Delta \cong \frac{kd\alpha}{\pi}\left\{\left(\frac{1}{\epsilon_r} - \mu_r\right)\left[\ln(\sqrt{\alpha^2-1}\ kd) + \gamma - 1\right]\right.$$

$$\left. + 2 Q_o(-\delta_\epsilon) - 2 Q_o(\delta_\mu)\right\} \tag{14b}$$

$$f_e(-\sqrt{n^2-\alpha^2}) \cong \frac{-2\sqrt{n^2-\alpha^2}\ kd}{\pi}\left\{\frac{1}{\epsilon_r}\left[\ln(\sqrt{\alpha^2-1}\ kd) + \gamma - 1\right]\right.$$

$$\left. + 2 Q_o(-\delta_\epsilon) - \ln(2\pi)\right\} \tag{14c}$$

When $\alpha \sim n$, Δ is very small and

$$\chi(\alpha) \simeq \frac{2kd}{\pi\sqrt{n^2-\alpha^2}} \left[(1-\alpha^2)\mu_r \left\{ \ln(\sqrt{\alpha^2-1}\ kd) + \gamma-1 \right\} \right.$$

$$+ n^2 \left\{ 2Q_o(-\delta\epsilon) - \ln(2\pi) \right\}$$

$$\left. - \alpha^2 \left\{ 2Q_o(\delta\mu) - \ln(2\pi) \right\} \right] \tag{14d}$$

$$\delta\epsilon = \frac{\epsilon_r - 1}{\epsilon_r + 1} \quad ; \quad \delta\mu = -\frac{\mu_r - 1}{\mu_r + 1} \quad ; \quad Q_o(z) = \sum_{m=1}^{\infty} z^m \ln(m) \tag{15}$$

and γ = Euler's constant 0.5772. Equation (14) is valid for $kd < 1$ as is found in many practical cases. For thicker slabs, one can employ the integral representation given in [2] directly.

2.4 Physical Interpretation and Analysis of The Field Expression

The transverse resonance condition for a conducting strip of finite width ℓ occurs when the total phase change for the TEM wave bouncing back and forth between the two ends of the strip $-2\chi(\alpha) + 2k\sqrt{n^2-\alpha^2}\ \ell$ is equal to an integer multiple of 2π; that is,

$$-2\chi(\alpha) + 2\ k\ell\sqrt{n^2-\alpha^2} = -2p\pi \tag{16a}$$

The first term is the phase accumulation resulting from the complete reflection of this wave from the two edges and the second term is the phase change across the transverse y dimension for the zig-zagging wave.

The particular values of $\alpha = \alpha_p$, $p = 1, 1, 2, \ldots$ that produce this resonance correspond to the modes on a microstrip structure. These can be determined by a numerical root finding scheme. However, the graphical representation of eq. 16a by Chang [1] helps depict the propagating and evanescent modes.

10

The report [1]'s figure number 4 is repeated here as Figure 3 for convenience.
Equation (16a) is rewritten as $F_p(k;\alpha)$

$$k\ell = F_p(k;\alpha) \ ; \ F_p(k;\alpha) = \frac{p\pi + \chi(\alpha)}{\sqrt{n^2 - \alpha^2}} \tag{16b}$$

Figure 3 shows the function $F_p(k\alpha)$ for $p = 0, 1, 2,\ldots$ as a function of α for a dielectric slab of premittivity $\varepsilon = 10\varepsilon_0$ and thickness d of 1.27 mm and desired resonant frequency 8GHz. $\alpha = \alpha(p)$ is then given by intersecting $k\ell$ with the set of curves $F_p(k,\alpha)$. Only a finite number of roots appear on the real α axis. In this case for $p = 0, 1, 2$ we have $\alpha = 3.05, 2.95, 1.075$. The rest appear as a continuous mode spectrum of the evanescent modes. In contrast, for the case of perfect magnetic walls (perfect cavity - no radiation), there are not only a fininte number on the real axis corresponding to propagating modes but also eq. (16b) gives an infinite set of discrete roots on the imaginary α axis corresponding to discrete evanescent modes which represent the reactive part of the probe impedance.
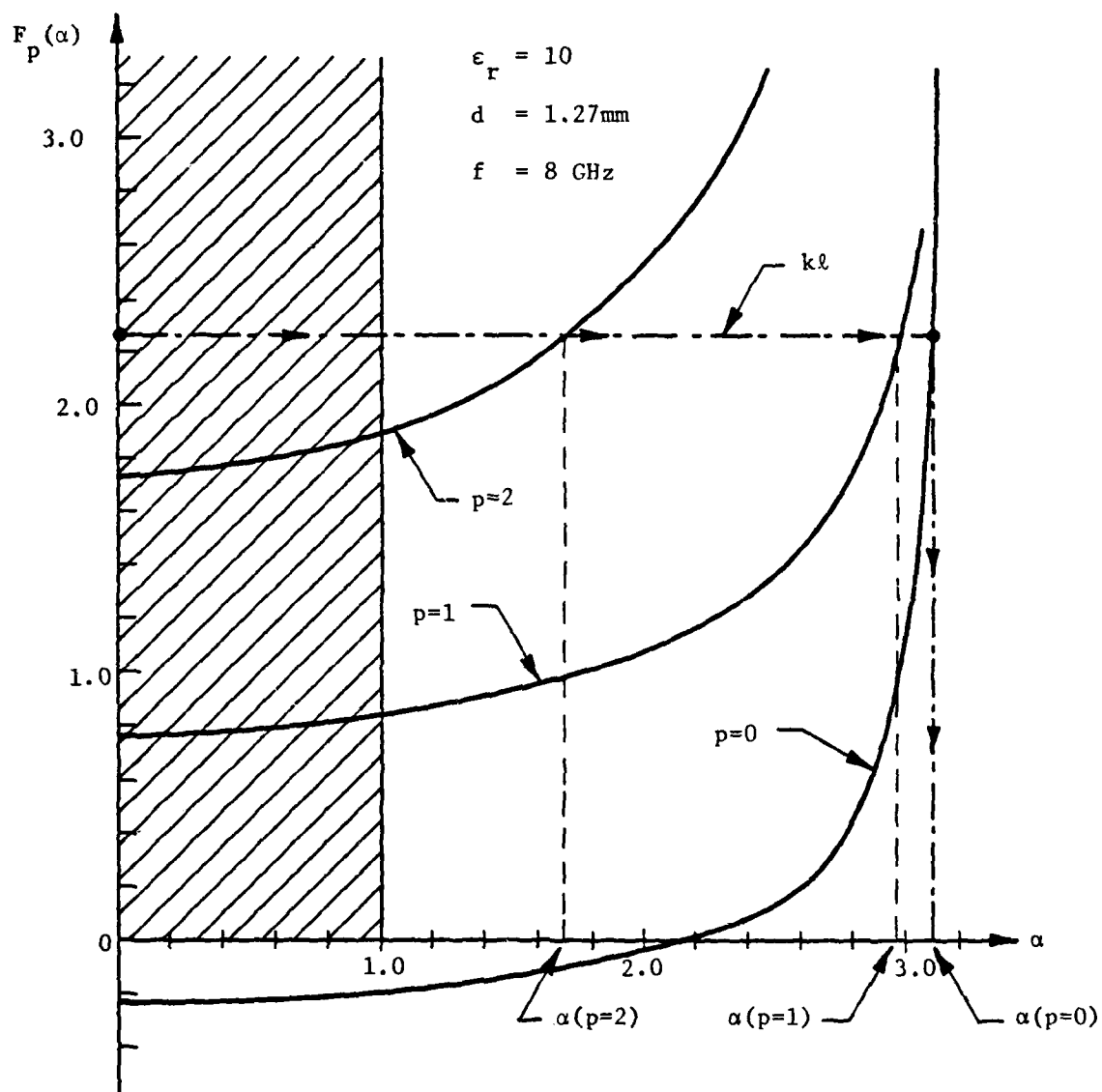
Figure 3. Graphical Method for determining the
propagating modes. (After Chang, D.C. [1]).

In addition, for the leaky radiating cavity the function $\chi(\alpha)$ has branch points at $\alpha = \pm 1$ and the path of integration is deformed upwards (for $x > x_o$) as shown in Figure 4a. The integration path then wraps around the branch cut as shown in Figure 4b. The infinite integral in eq. (12), would reduce to the sum of the branch cut integration and the sum of the residues at the poles on the real axis.

Equation (12) can be written as follows

$$E_z = A_o\left[\int\limits_{i\infty}^{o} f(\alpha)\ d\alpha + \int\limits_{0}^{1} f(\alpha)\ d\alpha\right]$$

$$+ 2\pi i\ A_o\ \sum_p (\text{residues at the poles on the real axis}) \qquad (17)$$

where

$$f(\alpha) = \frac{2e^{ik\alpha|x-x_o|}}{\sqrt{n^2-\alpha^2}}\ e^{ik\sqrt{n^2-\alpha^2}\ell}\left[\left(\frac{\Gamma_1(\alpha)}{\Delta_1} - \frac{\Gamma_2(\alpha)}{\Delta_2}\right)\cos\left(k\sqrt{n^2-\alpha^2}(y+y_o)\right)\right.$$

$$\left.+\left(\frac{\Gamma_1^2(\alpha)}{\Delta_1} - \frac{\Gamma_2^2(\alpha)}{\Delta_2}\right)e^{ik\sqrt{n^2-\alpha^2}\ell}\cos\left(k\sqrt{n^2-\alpha^2}\ (y-y_o)\right)\right] \qquad (18)$$

and

$\Gamma_1(\alpha)$, $\Delta_1(\alpha)$ are calculated for $\sqrt{\alpha^2-1} = -i\sqrt{1-\alpha^2}$

$\Gamma_2(\alpha)$, $\Delta_2(\alpha)$ are calculated for $\sqrt{\alpha^2-1} = +i\sqrt{1-\alpha^2}$ $\qquad (19)$

The poles of the equation are defined by eq. (16b). If $\alpha = \alpha_p$ defines the location of pole of order $p=0$, the residue at this pole is given as follows

$$\text{Residue} = 4\pi A_o\left[\frac{e^{ik\alpha|x-x_o|}\cos(k\sqrt{n^2-\alpha^2}\ y)\ \cos(k\sqrt{n^2-\alpha^2}\ y_o)}{(\sqrt{n^2-\alpha^2}\ \chi'(\alpha) + k\ell\alpha)}\right]_{\alpha\ =\ \alpha_p} \qquad (20)$$

13

Here the width ℓ of the patch is chosen such that only the dominant TM_{01} mode propagates.

In eq. (20),

$$\chi'(\alpha) = \frac{2kd}{\pi\sqrt{n^2-\alpha^2}} \left[\left\{ \mu_r(\gamma-1) + 2n^2 Q_0(-\delta_\varepsilon) - n^2 \ell n(2\pi) \right\} \frac{\alpha}{(n^2-\alpha^2)} \right.$$

$$- \left\{ \mu_r(\gamma-1) + 2Q_0(\delta_\mu) - \ell n(2\pi) \right\} \left\{ 2\alpha + \frac{\alpha^3}{(n^2-\alpha^2)} \right\}$$

$$+ \mu_r \left\{ \frac{\alpha}{(\alpha^2-1)} + \frac{\alpha \, \ell n(\sqrt{\alpha^2-1}\,kd)}{(n^2-\alpha^2)} \right\}$$

$$\left. - \mu_r \left\{ 2\alpha \ell n(\sqrt{\alpha^2-1}kd) + \frac{\alpha^3}{(\alpha^2-1)} + \frac{\alpha^3 \ell n(\sqrt{\alpha^2-\ell}kd)}{(n^2-\alpha^2)} \right\} \right] \tag{21}$$

The physical interpretation of the poles and branch cuts is as follows. The poles on the real axis correspond to the propagating modes which define the resonance for the patch. For a wide patch there may be more than one such guiding mode. In the case of perfect magnetic walls a series of poles occur on the imaginary axis. These correspond to the discrete evanescent modes in the cavity which add up to give the reactive part of the probe impedance (see Figure 5a). However, for the case of leaky magnetic walls when the reflection coefficient is no longer unity and is now given by eq. (14), the evanescent modes appear as the continuous mode spectrum in the form of the branch cut integration from $i\infty$ to o (see Figure 5b). If $\Gamma = 1$ in this region, then the discrete evanescent modes predicted by the cavity model can be obtained. When $\chi \neq 0$, α_p is obtained from

$$\sqrt{n^2 + \alpha_\rho^2} - \chi(i\alpha_p) = p\pi \tag{22}$$

and when $\chi = 0$, that is $\Gamma = 1$, α_p' is obtained from

$$\sqrt{n^2 + \alpha_p'^2} = p\pi \tag{23}$$

14

It can be shown analytically that for $d/\ell \ll 1$ the difference in the above two cases is immaterial for integration along the imaginary axis and we can then put $\Gamma = 1$ in this region.

Further, the modes which are guided down the patch leak out as spurious radiation at each bounce in the x direction. This radiation is represented by the branch cut integration from 0 to 1. The integrand $f(\alpha)$ given in eq. (18) is purely reactive. It can be shown analytically that this spurious radiation is of the order of kd which can be ignored since the resonant term is of the order of $1/kd$ at resonance.

Hence the field under the infinite microstrip patch antenna reduces to the residue at the pole corresponding to the propagating mode $p=0$ and the sums of the residues at the poles on the imaginary axis corresponding to the evanescent modes $p = 1, 2, \ldots$

$$E_z = 4\pi A_o \frac{\cos(k\sqrt{n^2 - \alpha^2}\, Y)\cos(k\sqrt{n^2 - \alpha^2}\, Y_o)e^{ikd|x-x_o|}}{(\sqrt{n^2 - \alpha^2}\, \chi'(d) + k\ell\alpha)} \Bigg|_{\alpha = \alpha_p = 0}$$

$$+ \frac{2\pi A_o}{k\ell} \sum_{p=1}^{\infty} \frac{e^{ik\alpha|x-x_o|}}{\alpha} \left[\cos(\tfrac{p\pi}{\ell}(Y + Y_o)) + (-1)^P\cos(\tfrac{p\pi}{\ell}(Y - Y_o))\right] \Bigg| \tag{24}$$

$$\alpha = \sqrt{n^2 - \left(\frac{p\pi}{k\ell}\right)^2}$$

3.0 TRUNCATED MICROSTRIP PATCH ANTENNA

Having established the entire spectrum of plane waves emanating from the exciting probe for an infinite patch, the patch can now be truncated to bounce these guiding and evanescent modes in the x direction. The geometry of the truncated patch is given in Figure 6. The length of the patch is h and the probe is located at (x_o, y_o).
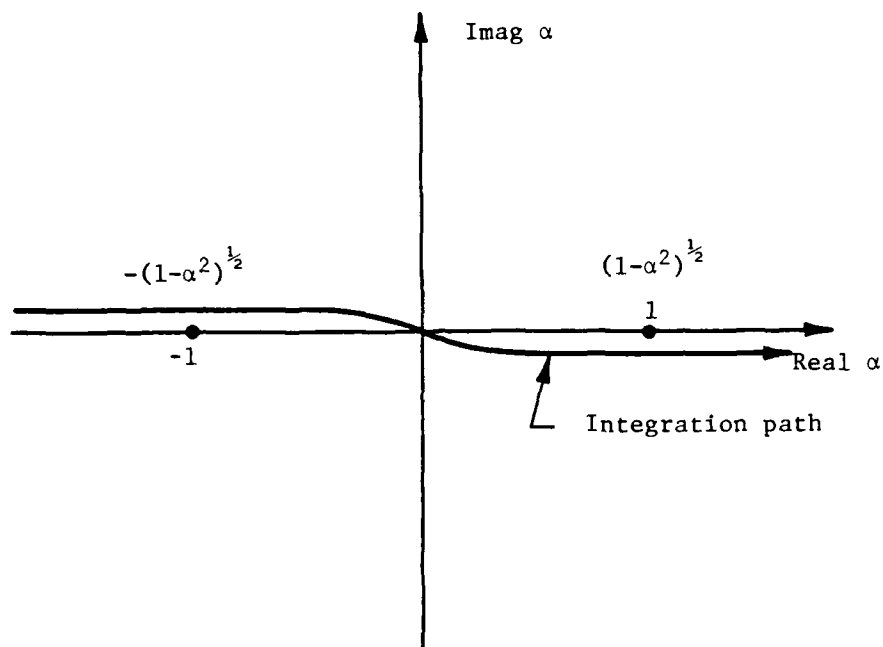
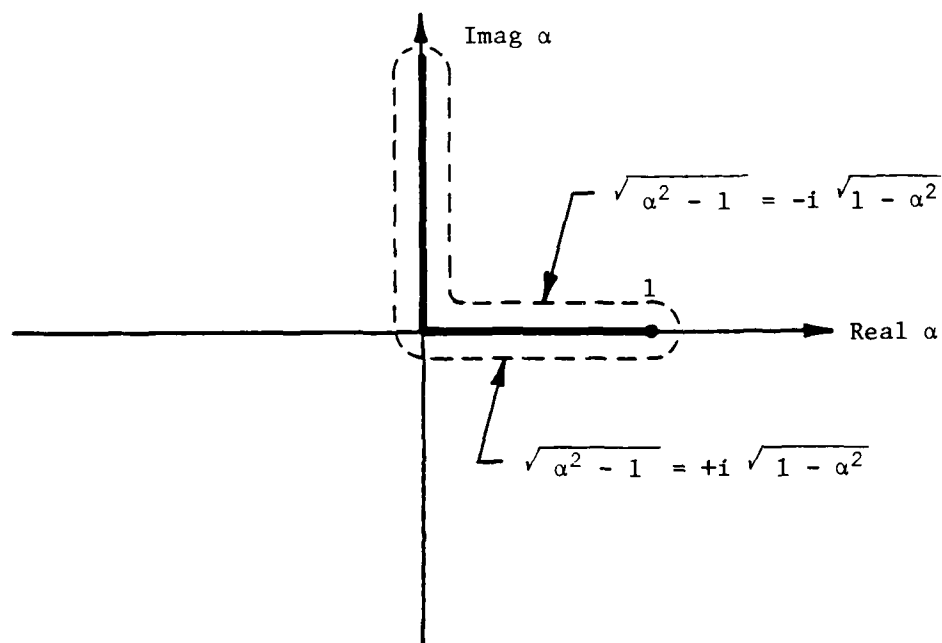Figure 4a. Deforming the path of integration.

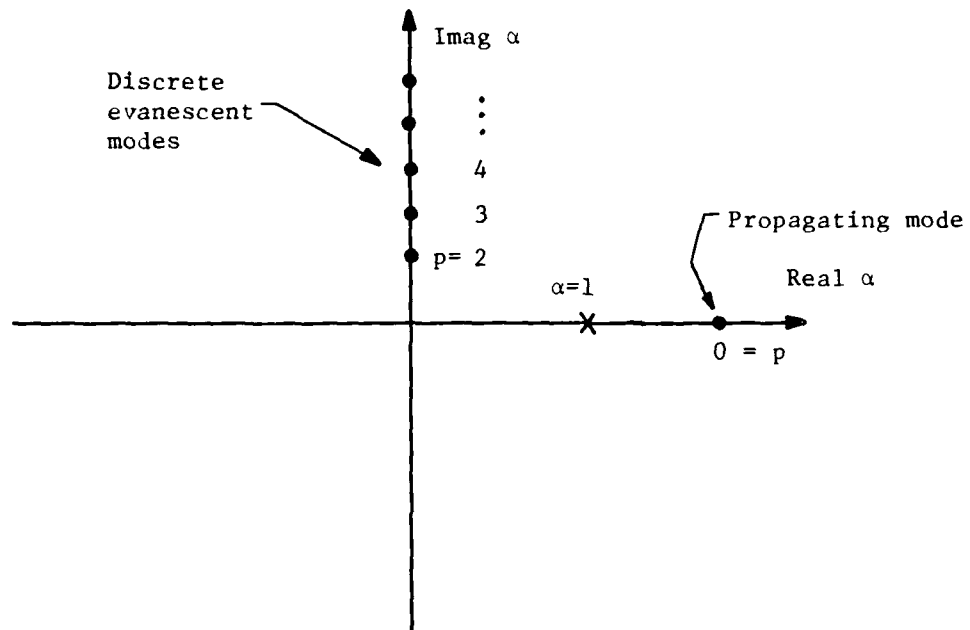Figure 4b. Branch cut and the path of integration for $x > x_o$.

Fig. 5a.   Propagating and evanescent modes for perfect magnetic walls.
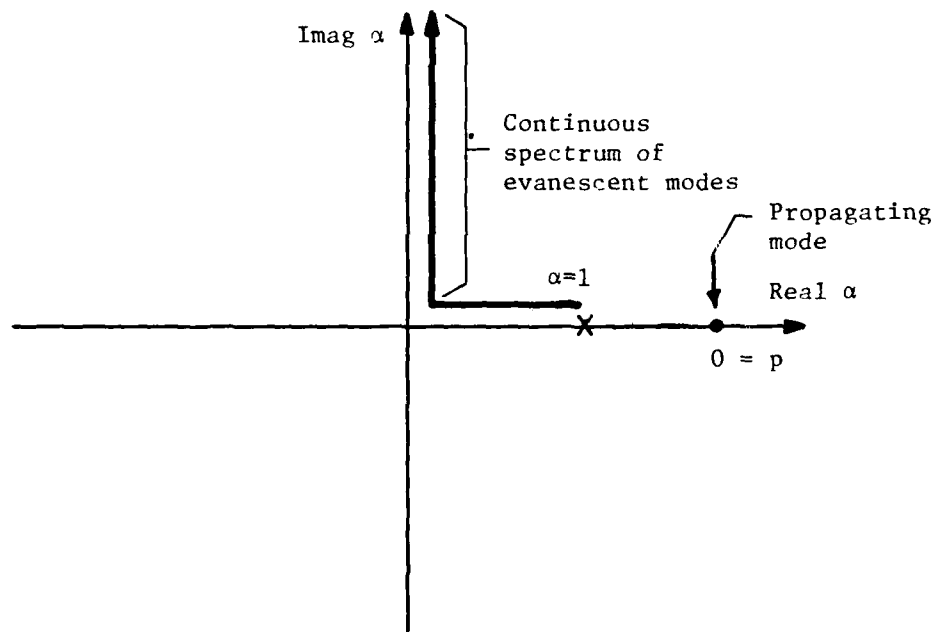

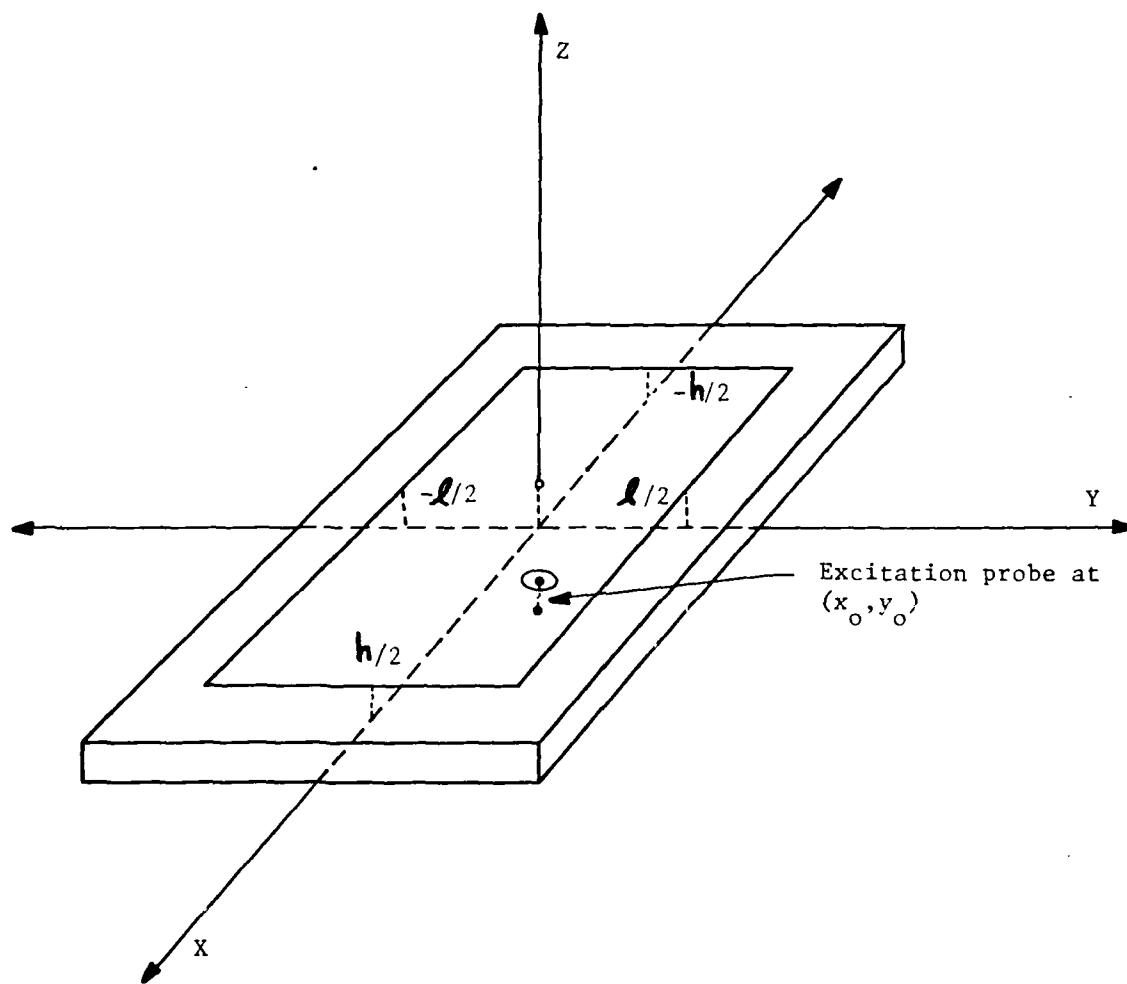Fig. 5b.   Leaky cavity with an angularly dependent reflection coefficient.

Fig. 6. Truncated microstrip patch antenna.

Bouncing the mode in the x direction would amount to expanding the term $e^{ik\alpha(x-x_o)}$ in eq. (18). This is equivalent to the sum of the incident waves and the waves travelling in the $\pm x$ directions, that is

$$e^{ik\alpha|x-x_o|} + Ce^{ik\alpha\left(\frac{h}{2} - x\right)} + De^{ik\alpha\left(x + \frac{h}{2}\right)} \tag{25}$$

As before the amplitudes C and D can be determined at h/2 and -h/2. In order to account for the bounces from the two end walls of a microstrip we need to replace exp $(ik\alpha|x-x_o|)$ in eq. (19) and (20) by

$$e^{ik\alpha|x-x_o|} + \frac{\Gamma(\sqrt{n^2-\alpha^2})e^{ik\alpha h}}{1-\Gamma^2(\sqrt{n^2-\alpha^2})e^{i2k\alpha h}} \left[\cos\left(k\alpha(x+x_o)\right)\right.$$
$$\left. + \Gamma(\sqrt{n^2-\alpha^2})\, e^{ik\alpha h}\, \cos\left(k\alpha(x-x_o)\right)\right] \tag{26}$$

$e^{ik\alpha|x-x_o|}$ in eq. (25) is replaced by eq. (26) to obtain the entire field under the truncated microstrip patch antenna.

4.0 INPUT IMPEDANCE TO PROBE-FED MICROSTRIP PATCH ANTENNAS

The electric field at the feed probe is effectively that averaged over the area of the probe, i.e.,

$$\langle E_z \rangle_a = \frac{1}{2\pi} \int_0^{2\pi} d\phi\ E_z\ (x,y)\ \Big|\ x = x_o + a\cos\phi,\ y = y_o + a\sin\phi \tag{27}$$

where a is the probe radius. Utilizing eqs. (24) and (26),

$$\langle E_z \rangle_a = \frac{4\pi A_o}{(\sqrt{n^2 - \alpha^2}\ \chi'(\alpha) + k\ell d} \left[1 + \frac{2\Gamma(\sqrt{n^2 - \alpha^2})e^{ik\alpha h}}{1-\Gamma^2(\sqrt{n^2-\alpha^2})e^{i2k\alpha h}} \right.$$
$$\left. \left\{ \cos(2k\alpha x_o) + \Gamma(\sqrt{n^2 - \alpha^2})e^{k\alpha h} \right\} \right]$$
$$+ \frac{4\pi i A_o}{k\ell} \sum_{\substack{p=2 \\ (even)}}^{\infty} \left[\frac{\cos(2k\alpha x_o) + e^{ik\alpha h}}{\sin(kah)} - \frac{1}{\left(\frac{2p\pi}{k\ell}\right)^2 - n^2} + \frac{1}{\left(\frac{2p\pi}{k\ell}\right)} \right]$$

19

$$+ \quad iA_o \left[\ln\left(\frac{8\pi^2 a^2}{\ell^2}\right) - \frac{2a}{\ell} \right] \tag{28}$$

and the input impedance would be

$$Z_{in} \simeq \frac{-<E_z>_a d}{I} \tag{29}$$

where d is the thickness of the substrate.

The above analysis has been based on a dynamic model and has not included the possibility of a resonant TM_{00} mode. The TM_{00} mode yields a basically uniform charge distribution on the patch and is associated with the static capacitance of the patch given by

$$C_{00} = \epsilon \frac{\ell h}{d} \tag{30a}$$

This capacitive reactance has to be added to eq. (29) to give the total input impedance for the patch.

$$Z_{in} = \frac{-<E_z>_a d}{I} - \frac{jd}{\omega \epsilon \ell h} \tag{30b}$$

5.0 THE LIMITING CASE OF PERFECT MAGNETIC WALLS AS A COMPARISON TO THE CAVITY MODEL.

The purpose of this section is to show that in the limit of perfect magnetic walls this theory reduces to the cavity model where the field is given by the sum of all modes in the x and y directions.

For perfect open circuit walls, for which there is no leakage outside the cavity,

$$\Gamma(\alpha) = 1 = \Gamma(\sqrt{n^2-\alpha^2}) \tag{31}$$

As before, we consider an infinitely long microstrip patch and establish all the propagating and evanescent modes. Substituting $\Gamma(\alpha) = 1$ in eq. (12).

$$E_z = A_o \int_{-\infty}^{\infty} \frac{e^{ik\alpha(x-x_o)}}{\sqrt{n^2-\alpha^2}} \left[e^{ik\sqrt{n^2-\alpha^2}\,(y-yo)} + \frac{2e^{ik\sqrt{n^2-\alpha^2}\ell}}{1-e^{i2k\sqrt{n^2-\alpha^2}\ell}} \left\{ \cos\left(k\sqrt{n^2-\alpha^2}\,(y+y_o)\right) \right. \right.$$

$$\left. \left. + e^{ik\sqrt{n^2-\alpha^2}\ell}\cos\left(k\sqrt{n^2-\alpha^2}\,(y-y_o)\right) \right\} \right] d\alpha \qquad (32)$$

Poles occur when

$$2\ k\sqrt{n^2-\alpha^2}\ell \ \ = 2p\pi \qquad (33)$$

Therefore,

$$E_z = 2\pi i A_o \sum_p \frac{e^{ik\alpha\left|x-x_o\right|}}{\sqrt{n^2-\alpha^2}} \left[\frac{2e^{ik\sqrt{n^2-\alpha^2}\ell}\left\{\cos\left(k\sqrt{n^2-\alpha^2}(y+yo)\right) + e^{ik\sqrt{n^2-\alpha^2}\ell}\cos\left(k\sqrt{n^2-\alpha^2}(y-yo)\right)\right\}}{\left(-e^{i2k\sqrt{n^2-\alpha^2}\ell}\right)\left(\frac{i2k\ell(-2\alpha)}{2\sqrt{n^2-\alpha^2}}\right)} \right]$$

$$E_z = \frac{2\pi Ao}{k\ell} \sum_p e^{ik\alpha\left|x-x_o\right|} \left[\frac{1}{\alpha e^{ik\sqrt{n^2-\alpha^2}\ell}} \left\{ \cos\left(k\sqrt{n^2-\alpha^2}(y+y_o)\right) + e^{ik\sqrt{n^2-\alpha^2}\ell} \right. \right.$$

$$\left. \left. \cos\left(k\sqrt{n^2-\alpha^2}\,(y-y_o)\right) \right\} \right]_{k\sqrt{n^2-\alpha^2}\ell \ = \ p\pi} \qquad (34)$$

Simplifying,

$$E_z = \frac{2\pi Ao}{k\ell} \sum_p \frac{e^{ik\alpha|x-x_o|}}{2\alpha \, e^{ip\pi}} \left[e^{\frac{ip\pi}{\ell} y_o} \left(e^{\frac{ip\pi}{\ell} y_o} + e^{\frac{-ip\pi}{\ell} y_o} e^{ip\pi} \right) \right.$$

$$\left. + e^{\frac{-ip\pi}{\ell} y} \left(e^{\frac{-ip\pi}{\ell} y_o} + e^{ip\pi} e^{\frac{ip\pi}{\ell} y_o} \right) \right] \qquad \alpha = \alpha(p) \tag{35}$$

This can also be obtained by setting $\Gamma(\alpha) = 1$ in eq. (24).

For p even

$$E_z = \frac{4\pi Ao}{k\ell} \sum_{p \text{ even}} \frac{e^{ik\alpha|x-x_o|}}{\alpha} \cos\left(\frac{p\pi}{\ell} y\right) \cos\left(\frac{p\pi}{\ell} y_o\right) \tag{36}$$

For p odd

$$E_z = \frac{4\pi Ao}{kl} \sum_{p \text{ odd}} \frac{e^{ik\alpha|x-x_o|}}{\alpha} \sin\left(\frac{p\pi y}{\ell}\right) \sin\left(\frac{p\pi}{\ell} y_o\right) \tag{37}$$

These eqs. (36) and (37) give the propagating and evanescent modes as the plane waves bounce in the y direction in an infinitely extending patch with perfect magnetic walls. Truncating the patch and expanding $e^{ik\alpha|x-x_o|}$ where
$\Gamma(\sqrt{n^2 - \alpha^2}) = 1$

$e^{ik\alpha|x-x_o|}$ is then replaced by

$$e^{ik\alpha|x-x_o|} + \frac{2e^{ik\alpha h}}{1-e^{i2k\alpha h}} \left\{ \cos\left(k\alpha(x+x_o)\right) + e^{ik\alpha h} \cos\left(k\alpha(x-x_o)\right) \right\} \tag{38}$$

$$k\sqrt{n^2-\alpha^2}\,\ell = p\pi$$

22

The sum in eq. (38) will be replaced by the function $\phi(\alpha)$.

This function $\phi(\alpha)$ should satisfy the following equations; the wave equation

$$\left(\frac{d^2}{dx^2} + k^2 \alpha^2\right) \phi = i2\alpha k\delta \ (x-x_o) \tag{39}$$

and the boundary condition

$$\phi'(\alpha) = 0 \qquad \text{at } x = \pm h/2 \tag{40}$$

Assuming a solution of the form

$$\phi(\alpha) = \Sigma \ A_n \cos\left(\frac{n\pi}{h/2} \ x\right) \text{ for } n = 1, 2... \tag{41}$$

which satisfies the orthogonality relation

$$\int_{-h/2}^{h/2} A_m \cos\left(\frac{m\pi}{h/2} \ x\right) \Sigma \ A_n \cos\left(\frac{n\pi}{h/2} \ x\right) \ dx = \text{constant for } m = n \tag{42}$$

substituting (41) into (42) we have

$$\frac{h}{2} \ A_m \left[k^2 \ \alpha^2 - \left(\frac{2m\pi}{h}\right)^2\right] = 2i\alpha k \cos\left(\frac{2m\pi}{h} \ x_o\right)$$

and

$$A_m = \frac{i4\alpha k}{h} \left[\frac{1}{k^2 \ \alpha^2 - \left(\frac{2m\pi}{h}\right)^2}\right] \cos\left(\frac{2m\pi}{h} \ x_o\right) \tag{43}$$

This gives,

$$\phi(\alpha) = \frac{i4\alpha k}{h} \sum_m \left[\frac{1}{k^2\alpha^2 - \left(\frac{m\pi}{h}\right)^2} \right] \cos\left(\frac{2m\pi}{h} x_0\right) \cos\left(\frac{2m\pi}{h} x\right)$$

(44)

Here α satisfies the relation $k\sqrt{n^2-\alpha^2}\,\ell = p\pi$

and for p even, where $p = 2p'$

$$k^2\alpha^2 = k^2 n^2 - \left(\frac{2p'\pi}{\ell}\right)^2$$

(45)

Therefore,

$$\phi(\alpha) = \frac{i4\alpha k}{h} \sum_m \frac{1}{k^2 n^2 - \left(\frac{2p'\pi}{\ell}\right)^2 - \left(\frac{2m\pi}{h}\right)^2} \cos\left(\frac{2m\pi}{h} x_0\right) \cos\left(\frac{2m\pi x}{h}\right)$$

(46)

and, for p even

$$E_z = \frac{i16\pi A_0}{\ell h} \sum_{p'} \sum_m \left[\frac{\cos\left(\frac{2p'\pi}{\ell} y_0\right) \cos\left(\frac{2p'\pi}{\ell} y\right) \cos\left(\frac{2m\pi}{h} x_0\right) \cos\left(\frac{2m\pi}{h} x\right)}{k^2 n^2 - \left(\frac{2p'\pi}{\ell}\right)^2 - \left(\frac{2m\pi}{h}\right)^2} \right]$$

(47)

Averaging the input field over the area of the probe we have,

$$\langle E_z \rangle_a = \frac{i16\pi A_0}{\ell h} \sum_{p'} \sum_m \left[\frac{\cos\left(\frac{2p'\pi}{\ell} y_0\right) \cos\left(\frac{2m\pi}{h} x_0\right)}{k^2 n^2 - \left(\frac{2p'\pi}{\ell}\right)^2 - \left(\frac{2m\pi}{h}\right)^2} \right.$$

$$\left. \int_0^{2\pi} \cos\left(\frac{2m\pi}{h} (x_0 + a\cos\phi)\right) \cos\left(\frac{2p'\pi}{\ell} (y_0 + a\sin\phi)\right) d\phi \right]$$

(48)

24

For p' even, the integral in (48) becomes

$$\int_0^{2\pi} \cos\left(\frac{2m\pi}{h}(x_0 + a\cos\phi)\right)\cos\left(\frac{2p'\pi}{\ell}(y_0 + a\sin\phi)\right)d\phi$$

$$= \cos\left(\frac{2m\pi}{h}x_0\right)\cos\left(\frac{2p'\pi}{\ell}y_0\right)\int_0^{2\pi}\cos\left(\frac{2m\pi}{h}a\cos(\phi)\right)\cos\left(\frac{2p'\pi}{\ell}a\sin(\phi)\right)d\phi \quad (49)$$

$$= \frac{1}{2}\cos\left(\frac{2m\pi}{h}x_0\right)\cos\left(\frac{2p'\pi}{\ell}y_0\right)\int_0^{2\pi}\left[\cos\left(\frac{2m\pi}{h}a\cos(\phi) + \frac{2p'\pi}{\ell}a\sin(\phi)\right)\right.$$

$$\left. + \cos\left(\frac{2m\pi}{h}a\cos(\phi) - \frac{2p'\pi}{\ell}a\sin(\phi)\right)\right]d\phi$$

$$= \frac{1}{2}\cos\left(\frac{2m\pi}{h}x_0\right)\cos\left(\frac{2p'\pi}{\ell}y_0\right)\int_0^{2\pi}\left[\cos\left\{\sqrt{u^2+v^2}\,a\cos(\phi+\phi_0)\right\}\right.$$

$$\left. + \cos\left\{\sqrt{u^2+v^2}\,a\cos(\phi-\phi_0)\right\}\right]d\phi$$

$$= \cos\left(\frac{2m\pi}{h}x_0\right)\cos\left(\frac{2p'\pi}{\ell}y_0\right)J_0\left(\sqrt{u^2+v^2}\,a\right) \quad (50)$$

where

$$u = \frac{2\pi m}{h}; \quad v = \frac{2p'\pi}{\ell}; \quad \phi_0 = \sin^{-1}\left(\frac{v}{\sqrt{u^2+v^2}}\right) \quad (51)$$

Substituting eq. (50) into eq. (48),

$$\langle E_z\rangle_a = \frac{i16\pi A o}{\ell h}\sum_{p'}\sum_m\frac{\cos^2\left(\frac{2p'\pi\,y_0}{\ell}\right)\cos^2\left(\frac{m\pi\,x_0}{h}\right)}{k^2n^2 - \left(\frac{2p'\pi}{\ell}\right)^2 - \left(\frac{2m'\pi}{h}\right)^2}\,J_0\left(\sqrt{\left(\frac{2m\pi}{h}\right)^2 + \left(\frac{2p'\pi}{\ell}\right)^2}\,a\right) \quad (52)$$

so that the input impedance is given by

$$Z_{in} = - \frac{i8\omega\mu d}{\ell h} \sum_{p'} \sum_{m} \frac{\cos^2\left(\frac{2p'\pi}{\ell} y_o\right) \cos^2\left(\frac{m\pi}{h} x_o\right)}{k^2 n^2 - \left(\frac{2p'\pi}{\ell}\right)^2 - \left(\frac{2m'\pi}{h}\right)^2} \cdot J_o\left(\sqrt{\left(\frac{2m\pi}{h}\right)^2 + \left(\frac{2p'\pi}{\ell}\right)^2} a\right)$$

(53)

The modes corresponding to p' and m are the same as that obtained in the cavity model. The Bessel function is the converging factor similar to G_{mn} in [6].

6.0 RESULTS

The input impedance for a rectangular patch of dimension ℓ = 6.858 cm and h = 4.14 cm mounted on a grounded dielectric of thickness d = 0.1588 cm and ϵ_r = 2.5 and excited by a probe of diameter 2a = 0.132 cms has been obtained using eqs. (29) and (30a). This is shown in Figure 7 as a function of frequency. The resonant resistance has been compared with that obtained by Carver and Coffey [10]. There is a 1% difference in the resonant frequencies obtained by the two theories. This can be explained as follows.

From the form of the reflection coefficient $\Gamma(\alpha)$ one can define the apparent end admittance of the microstrip structure as

$$Y(k,\alpha) = Y_o \frac{1 - \Gamma(\alpha)}{1 - \Gamma(\alpha)}$$

where $Y_o = \left(\frac{120\pi d}{n}\right)^{-1}$ is the characteristic admittance of the TEM wave in a parallel-plate waveguide. It suffices to note that the end admittance in general is a function of both frequency and angle of incidence. Nevertheless, for thin slabs, it can be approximated by the value at normal incidence at the end walls x = 0 and h. Hence the concept of a constant end admittance independent of the angle of incidence as in the cavity model has merit in this situation provided one recognizes the dynamic nature of the wall admittance.

26

Now, since the magnitude of the reflected wave is very close to unity we can show that

$$G = (gY_o)\ell = \nu\left(\frac{\ell}{\lambda_o}\right) \text{ where } \nu = \frac{ng}{60 \ kd}$$

The real part g of the normalized admittance varies linearly with kd so that g is now independent of the frequency. When g is plotted as a function of kd shown in Figure 8 (repeated from [1]), ν is determined by the slope of g and is 8×10^{-3}. On the other hand, the conventional theory which assumes that the end conductance can be calculated approximately from an open slot radiation in the absence of the substrate gives a slope of 8.33×10^{-3}. The error in omitting the surface wave radiation is typically of the order given by $(1 - \varepsilon_r^{-1})kd$ and is not significant when the substrate is thin.

As for the end susceptance of a microstrip of width ℓ, we can first define an equivalent length $\Delta\ell$ of an open circuit according to

$$B = (bY_o)\ell = \omega\varepsilon_r\varepsilon_o\Delta\ell \text{ where } \frac{\Delta\ell}{d} = \left(\frac{b}{nkd}\right)\frac{1}{d}$$

which is also plotted in Figure 8. Unlike the quasi-static theory which gives a result independent of frequency, the dynamic nature of our result is very explicit. Experimental results by Johnk and Chang [1] show that the Wiener-Hopf theory properly incorporates the high frequency effects into the modeling of the open end susceptance whereas the static approach is inadequate. An especially encouraging result of this is the fact that the incorporation of the angle of incidence in the Wiener-Hopf reflection coefficient produces a susceptance that is in excellent agreement with the experimental results.

In view of the above discussion it is obvious that the discrepancy between the two results shown in Figure 7 arises due to the difference the wall susceptance used by the two theoretical models. Further, the dynamic nature of the wall susceptance makes the present theory more appropriate for millimeter wavelength antennas.

Figures 9 and 10 show the resonant resistance and reactance for the dominant mode as the substrate thickness varies. As expected the resonant frequency shifts and the beamwidth increases with increasing electrical thickness.

ℓ = 6.858 cm

h = 4.14 cm

ϵ_r = 2.5

d = 0.1588 cm

a = 0.066 cm

(x_o, y_o):(1.054,0)
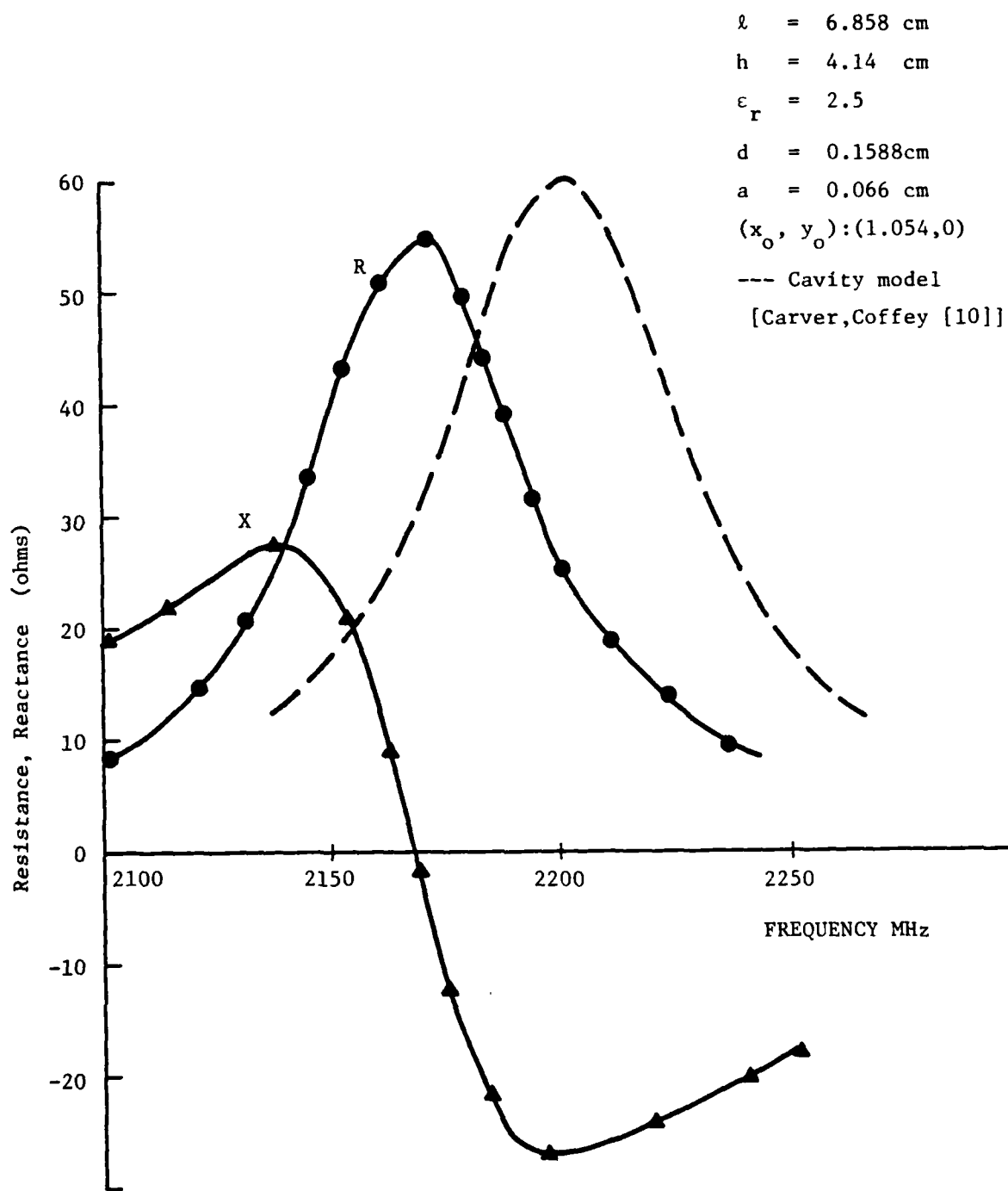
--- Cavity model

[Carver,Coffey [10]]

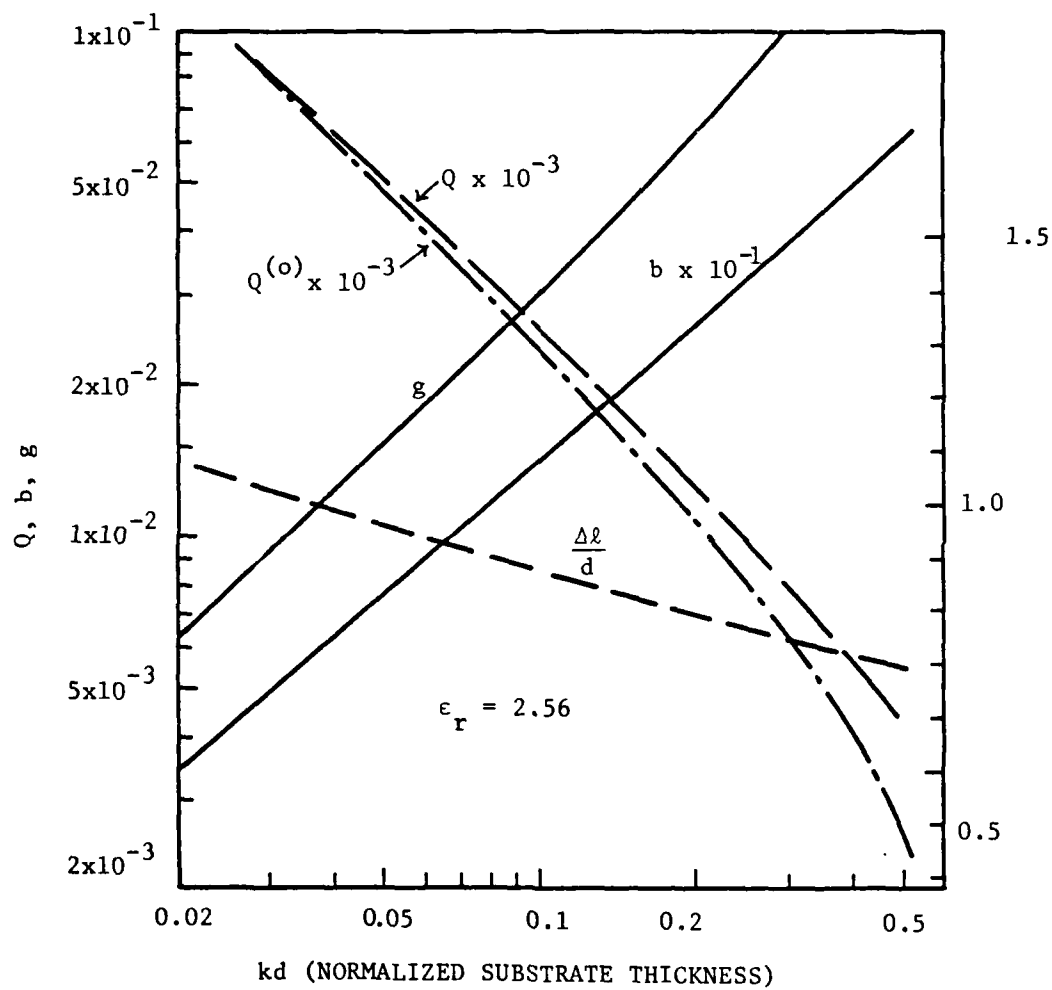Figure 7. Input Impedance to Patch vs. Frequency.

Figure 8. Plot of Real Part of Normalized Admittance
vs. Normalized Substrate Thickness.
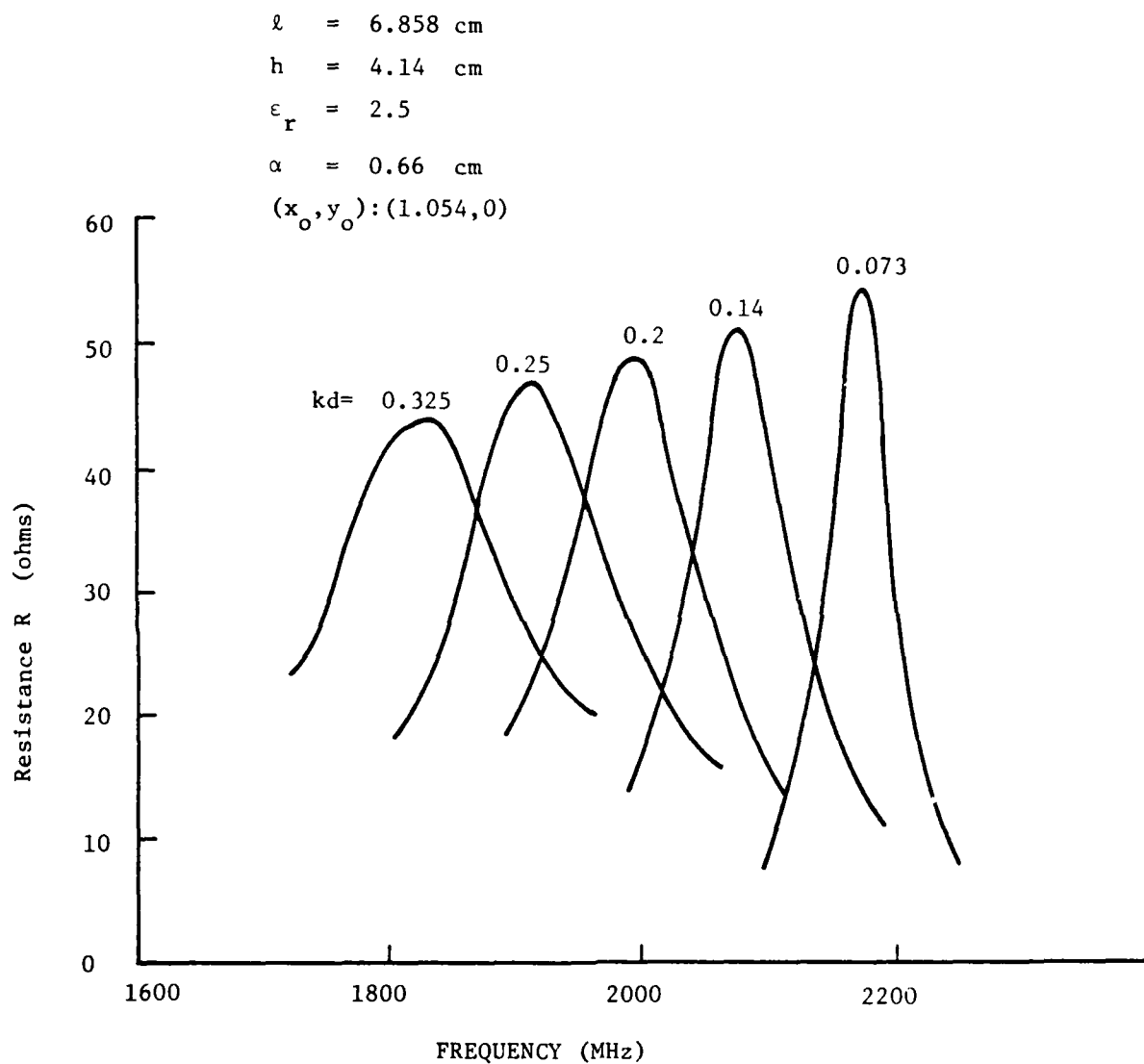(After Chang, D.C. [1]).

Figure 9. Resonant resistance vs. frequency.

ℓ = 6.858 cm

h = 4.14 cm

ε_r = 2.5
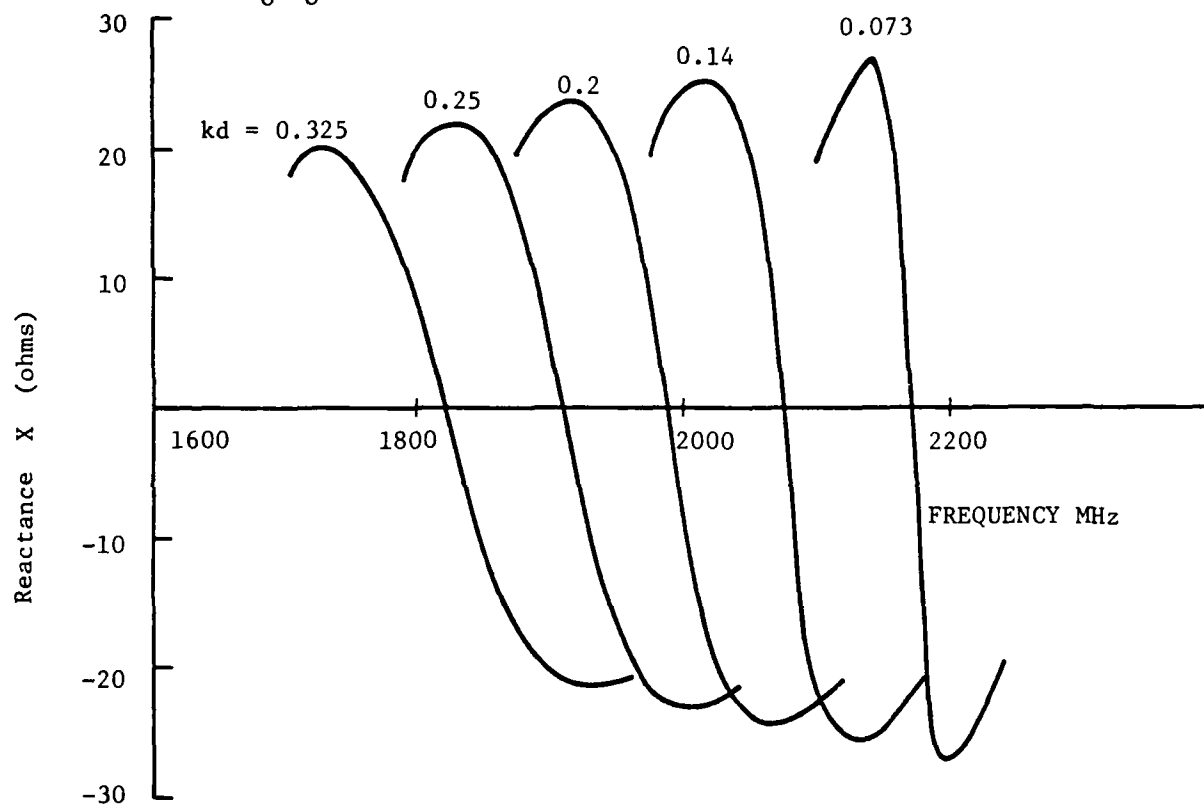
a = 0.066 cm

(x_o, y_o) = (1.054, 0)

Figure 10. Resonant reactance vs. frequency.

7.0 CONCLUSION

This report has presented a general theory for the analysis of the input impedance to a probe-fed microstrip patch antenna where the entire spectrum of plane waves emanating from the exciting probe has been considered and an angularly dependent wall reflection coefficient has been incorporated. The primary emphasis to its application is for the case of millimeter antennas where the substrate is electrically thick and makes it necessary to include the dispersion effects of the dielectric.

It is seen here that there are two kinds of waves which originate from the probe; those which are evanescent and decay in the vicinity of the probe therefore constituting the reactive part of the impedance and those which propagate down the patch and are the guiding modes. The guiding modes are discrete and finite in number for a given patch size and desired frequency of operations whereas the evanescent modes form a continuous spectrum. Further, the magnitude of the spurios radiation which leaks out of the cavity as the entire spectrum of plane waves bounce back and forth has been analytically estimated to be of the order of kd. The continuous spectrum of evanescent modes for the thick substrate or leaky walls is in contrast to the case of the perfect magnetic walls for which it can be shown analytically and confirmed by preliminary numerical analysis that the evanescent modes, like the propagating modes, are discrete. Hence the total field reduces to merely calculating the residues at the poles corresponding to all the modes since there is no (by assumption) radiation from the cavity. Although this assumption of discrete modes is also reasonable for substrates which are electrically thin, the radiation has to be accounted for in substrates which are electrically thick as in the case of millimeter wave microstrip antennas. Analytically it is shown that for the limiting case of perfect magnetic walls this general theory reduces to a form similar to that obtained in the cavity model. In order to do this, the single summation in eqs. (34) and (35), which includes the entire spectrum, was made to take the form of the familiar double summation which appears in the cavity model analysis. It should therefore be emphasized that establishing the mode spectrum for an infinitely long patch and then bouncing these modes for the truncated patch not only gives all the modes in both directions under the patch but also makes the numerical and mathematical analysis simpler.

REFERENCES

1. Chang, D. C. "Analytical theory of an unloaded rectangular microstrip patch", IEEE Trans. Ant. Prop., Vol. AP-29, No. 1, Jan. 1981.

2. Chang, D. C. and Kuester E. F. "Total and partial reflection from the end of a parallel plate waveguide with an entended dielectric slab", Rad. Sci. Vol. 16, No. 1, pp. 1-13, Jan-Feb 1981.

3. Kuester, E. F., Johuk, R. T. and Chang, D. C. "The thin substrate approximation for reflection from the end of a slab-loaded parallel-plate waveguide with application to microstrip patch antennas", (To be published in IEEE Trans. Ant. Prop., 1982).

4. Munson, R. E. "Corner fed microstrip antennas and microstrip phased arrays", IEEE Trans Art. Prop. Vol. AP-22, pp. 74-78, Jan. 1974.

5. Denneryd, A. G. "Linearly polarized microstrip antennas", IEEE Trans. Art. Prop., Vol. AP-24, pp. 848-851, Nov. 1976.

6. Lo, Y. T., Soloman, D. and Richards, W. F. "Theory and experiment on microstrip antennas", IEEE Trans. Art. Prop. AP-27 (1979) pp. 137-146.

7. Denneryd, A. G. and Lind A. G. "Extended analysis of rectangular microstrip resonator antennas", IEEE Trans. Art. Prop., Vol. AP-27, pp. 846-849, Nov. 1979.

8. Carver, K. R. "Input impedance to probe fed microstrip antennas", Proc. Int. Symp. Ant. Prop., June 1980.

9. Carver, K. R. and Venkataraman, J. "Input impedance to microstrip antennas over thick substrates", Proc. Rad. Sci. Meeting, Jan. 1981, pp 123.

10.   Carver, K.R. and Coffey, E.L. "Theoretical investigation of the microstrip antenna", Physical Science Laboratory, New Mexico State University, Las Cruces, New Mexico, Technical Report PT-00929, Jan. 23, 1979.

11.   Johnk, B. and Chang, D.C., "Experimental investigation of the end admittance of an open microstrip with application to microstrip patch antenna", paper presented at the National Radio Science Meeting, 13-15 Jan. 1982, Boulder Colorado.